Numerical simulation of runaway electrons generation in sulfur hexafluoride

D. Levko[a] and Ya. E. Krasik
Department of Physics, Technion, 32000 Haifa, Israel

(Received 17 August 2011; accepted 28 November 2011; published online 12 January 2012)

The results of the numerical simulation of the generation of runaway electrons in sulfur hexafluoride are presented. It is shown that the emission of the runaway electrons occurs from the cathode and its vicinity. The generation of these electrons is terminated because of the formation primarily by negative ions of a virtual cathode which causes the field emission to be screened. The simulations showed that the virtual cathode consists mainly of negative ions and cannot be an effective source of runaway electrons. In addition, the results of the simulations showed that the parameters of the runaway electrons depend on the amplitude and rise-time high-voltage pulse and gas pressure. © *2012 American Institute of Physics*. [doi:10.1063/1.3676256]

I. INTRODUCTION

Recent interest in the properties of pulsed high-voltage (HV) and high-current discharges in gas mixtures based on electronegative sulfur hexafluoride (SF_6) has been stimulated by the various applications of this gas in electronic, spark gap switches, and pulsed gaseous lasers.[1] However, the phenomena governing this type of discharge are not clearly understood yet. In Refs. 2–4, it was reported that the HV discharges are accompanied by the generation of runaway electrons (RAE), which was supposed to play a major role in the discharge formation. Namely, it was considered that the RAE generate efficiently secondary ions and electrons producing gas pre-ionization during their propagation toward the anode. These secondary electrons participate in ionization processes, forming the plasma that shorts the cathode-anode (CA) gap.

Numerical simulation studies of RAE generation in SF_6 gas were carried out by Yakovlenko *et al.*[5,6] In these simulations, one dimensional Particle-in-Cell (1D PIC) code was implemented for planar CA geometry. The potential difference between the cathode and anode φ_{CA} was considered to be a constant value. In addition, the model neglected the influence of the space charge of the secondary electrons and positive and negative ions generated in the CA gap on the electric field distribution inside the CA gap. The results of this modeling showed that at large CA gaps and at $E/P > 94$ V/(Torr·cm) one obtains the Townsend mechanism of ionization. Here E is the electric field and P is the gas pressure. In this case, the largest energy of electrons reaching the anode is $\varepsilon_e \ll e\varphi_C$, where e is the electron charge and φ_C is the cathode potential. In the opposite case, i.e., when $E/P < 94$ V/Torr·cm, electrons were mainly attached to the SF_6 molecules.

The experimental research of RAE generation in SF_6 during the nanosecond discharge was carried out by Baksht *et al.*[7] It was found that an increase in the gas pressure leads to the increase in time delay in the gap breakdown and RAE pulse duration and to the decrease in the amplitude of the RAE beam current. Also, it was shown that the increase in the voltage amplitude (keeping the gas pressure constant) leads to the decrease in RAE pulse duration.

In this paper, the results of a 1D PIC numerical simulation of RAE generation in SF_6 gas in a non-uniform and time-varying electric field which accounts self-space charged particles in CA gap are presented. It is shown the beam of RAE consist of electrons emitted from the cathode and generated in the cathode's vicinity. The generation of these electrons is terminated because of the formation mainly by generated negative ions of a virtual cathode (VC), which screens field emission (FE). It is shown that the parameters of RAE depend on the HV pulse rise time and amplitude, and on gas pressure. In addition, it was found that the VC consisting mainly of negative ions cannot be considered as an effective source of RAE.

II. NUMERICAL MODEL

For simulation of RAE generation in SF_6 gas, a 1D PIC numerical code described in details in Ref. 8 was used. A modeled diode consists of two coaxial cylinders: an internal cathode with the radius of $r_{CA} = 3$ μm and length of 1 cm, and an anode with $r_{CA} = 1$ cm. This diode configuration allows one to consider the cathode electric field enhancement that is typical for diodes with a blade-like cathode and planar anode. In addition, both the elastic[9] and inelastic collisions between electrons and SF_6 molecules were considered in the Monte-Carlo subroutine. The inelastic processes[9,10] were accounted for using a cross section of the excitation of the first electronic level σ_{ex}, ionization σ_{ion}, excitation of the first vibrational level σ_v, and an electron attachment σ_{att}. In each process of molecule ionization, one electron-ion pair was generated. The newly generated secondary electrons were added to the primary electrons. The initial velocities of the secondary electrons and ions are assumed to be zero, and their location is determined by the coordinate of the primary ionizing electron. An electron's attachment to a molecule is a very important process in electronegative gas because it influences the propagation of the electron avalanche. In the simulation, the attachment process leads to the disappearance of the electron from the radial-velocity phase space and to the addition of the negative ion SF_6^- with zero initial velocity

[a]Electronic mail: dlevko@physics.technion.ac.il.

with the coordinates of this primary electron. The ions' SF_6^+ and SF_6^- propagation was taken into account in the model as well. It is important to note that the SF_6^- propagation is extremely important. Indeed, the simulations showed that neglecting it leads to the accumulation of a negative charge at some locations, which leads to an unstable solution. The lifetime of SF_6^- is $\sim 2.5 \cdot 10^{-7}$ s,[11] which is much larger than the considered HV pulse rise times. Therefore, the process of detachment of electrons from SF_6^- was neglected.

The radial potential distribution was calculated at the beginning of each time step, solving a 1 D Poisson equation for cylindrical geometry for new electrons and ion space charge distributions and for new cathode and anode boundary conditions: $\varphi_c = -\varphi_0 \sin(2\pi t/T)$, $\varphi_a = 0$. Here, φ_0 is the maximal cathode potential whose value was varied in the simulations: 80 or 120, or 160 kV. The rise time of the cathode potential was determined as $T/4$, where T is the period that was varied: 1 or 1.5, or 2 ns.

The electron emission from the cathode was governed by FE described by the Fowler-Nordheim (FN) law.[11] The quantity dN_{em} of electrons with zero velocity and zero (cathode) coordinates was added to the simulations at the beginning of each time step according to the FN law. The value of dN_{em} was determined as $dN_{em} = j_{FN} \cdot S \cdot dt/e$, where j_{FN} is the electron current density, dt is the time step, e is the electron charge, and S is the cathode surface area.

III. RESULTS AND DISCUSSION

Simulations showed that the injection of the first electron into the CA gap as a result of FE occurs at the time when the electric field at the cathode is $E_c \approx 2 \times 10^7$ V/cm. For given d_{CA}, the value of E_c is obtained for some value of the cathode potential φ_c which does not depend on the type of the gas, its pressure, or the HV pulse rise time. However, the change in T changes the time t_0 when the value of φ_c is reached. For example, for $r_{CA} = 1$ cm, $T = 1$ ns, and $P = 10^5$ Pa one obtains $\varphi_c \approx -44$ kV and $t_0 \approx 60$ ps.

In preceding research,[8] where a similar coaxial nitrogen (N_2)-filled diode was considered, it was shown that the process of RAE generation is strongly influenced by the formation of the VC. The VC was formed in the location where the spatial separation between electrons and ions occurred. The main part of the electrons in the VC location had energies smaller than the ionization potential of N_2 ($I_{N2} \approx 15.58$ eV), and these electrons cannot generate new electron-ion pairs. In addition, the ions did not propagate significantly toward the VC to neutralize it because of the short rise time of the cathode potential.

The ionization potentials of SF_6 ($I_{SF_6} \approx 16$ eV) and N_2 gases do not differ significantly from each other. Nevertheless, the value of σ_{ion} for SF_6 is larger than for N_2. For example, in SF_6 the largest value of $\sigma_{ion} \approx 7.6 \cdot 10^{-16}$ cm^2, while in N_2 $\sigma_{ion} \approx 2.6 \cdot 10^{-16}$ cm^2, i.e., for an equal electron temperature, the rate of ionization in SF_6 is larger than in N_2. Also, SF_6 gas has an additional source of inelastic losses of electron energy, namely, the electrons' attachment to neutrals. This process decreases the number of low-energy electrons and, respectively, increases the time of the gas gap breakdown with dense plasma formation. In addition, one can consider that SF_6^- ions are almost immovable during hundreds of picoseconds, and the mobility of SF_6^- is equal to that of SF_6^+ in the same conditions. These peculiarities of the SF_6 gas make the processes responsible for VC formation in SF_6 and in N_2 different. Indeed, only the beginning of the VC formation in SF_6 gas is similar to that in N_2 gas, forming a separation between slow positive ions and fast electrons. When the space charge of SF_6^+ reaches a large value, the separation terminates and one obtains three regions of space charge distribution. These are: the region with an excess of SF_6^+, the region with an excess of electrons and SF_6^-, and the region of quasi-neutral plasma. This charge separation influences the potential distribution [see Fig. 1(a)] significantly. The formation of the potential well OK*A [see Fig. 1(a)] causes the accumulation of electrons with $\varepsilon_e < I_{SF_6}$ in the K* vicinity. These electrons attach effectively to neutrals-generating ions SF_6^- [see

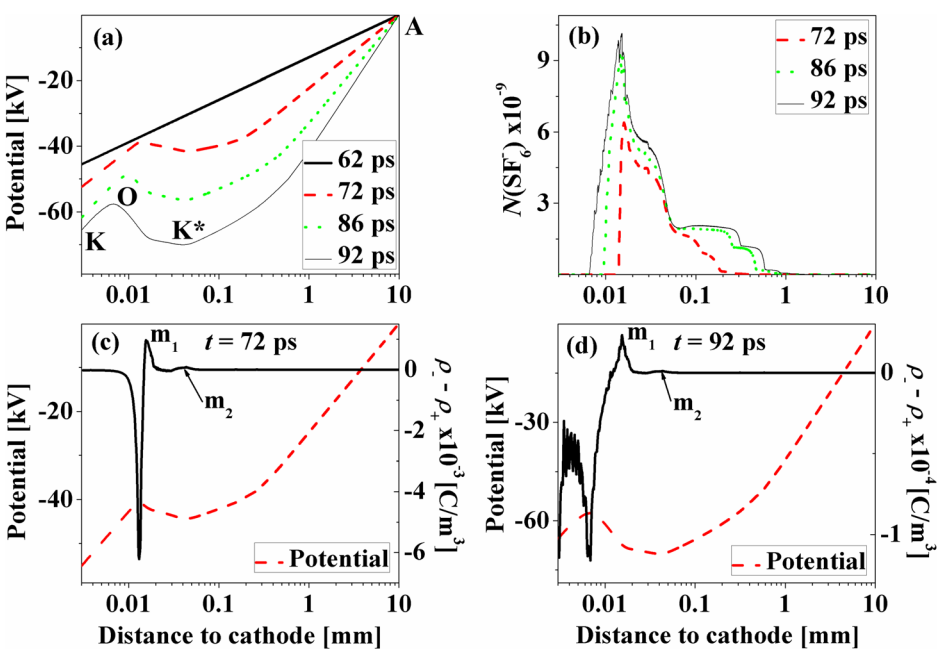

FIG. 1. (Color online) Distributions of potential (a), of negative ions SF_6^- (b), and of difference between negative and positive charge densities (c, d) in the CA gap at different times; $\varphi_0 = 120$ kV, $T = 1$ ns, $P = 10^5$ Pa.

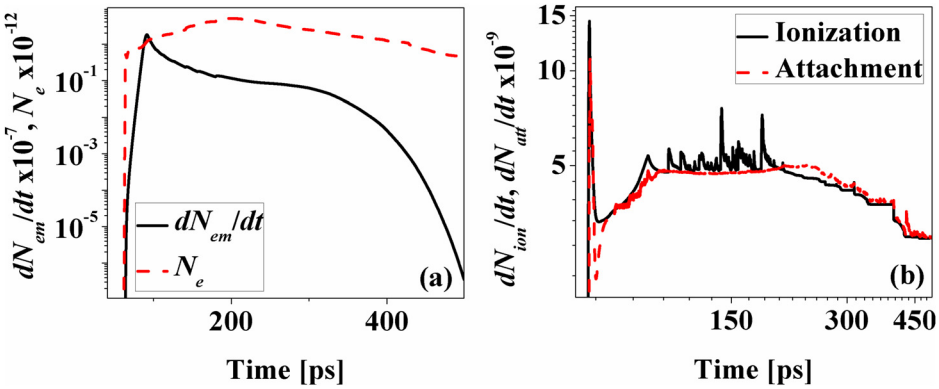

FIG. 2. (Color online) (a) Time dependence of the emitted dN_{em}/dt and total number of the electrons N_e in the CA gap; (b) time dependence of the numbers of ionizations and attachments per time step; $\varphi_0 = 120$ kV, $T = 1$ ns, $P = 10^5$ Pa.

Fig. 1(b)] because of the large value of σ_{att} for slow electrons (for example, $\sigma_{att} \approx 4 \times 10^{-14}$ cm^2 at $\varepsilon_e \approx 10^{-2}$ eV and $\sigma_{att} \approx 10^{-21}$ cm^2 at $\varepsilon_e \approx 0.9$ eV). The accumulation of SF_6^- ions in the K* location leads to the VC formation at that region. The distributions of difference between densities of negative and positive space charges at $t = 72$ and $t = 92$ ps are shown in Figs. 1(c) and 1(d). One can see three extreme maxima in these distributions. The minimum corresponds to the excess of ions [see point O in Fig. 1(a)] and the maximum m_2 corresponds to the location where the VC is formed. Point m_2 contains more electrons and SF_6^- ions than SF_6^+ ions. The maximum m_1 corresponds to the location where the SF_6^- ion density reaches the largest value [see Fig. 1(b)]. Comparing Figs. 1(c) and 1(d), one can see that at $t = 92$ ps the maximum with SF_6^+ ion density shifts toward the cathode. The maximum of SF_6^- ion density also shifts toward the cathode but less than the maximum of SF_6^+ ion density. Also, one can see an increase in the values of both the maxima. The shift of SF_6^+ ions toward the cathode is caused by the ions' acceleration by a large electric field in the cathode vicinity. This shift leads to an increase in the electric field in this location and, respectively, to an increased ionization rate due to the increased FE and electron energy. The SF_6^- ions are formed in the region with a smaller electric field and cannot shift toward the anode as quickly as SF_6^+ shift toward the cathode. Moreover, these negative ions shift slightly toward the cathode as a result of their attraction to SF_6^+.

The number of emitted electrons per time step dN_{em}/dt is presented in Fig. 2(a). The increase in dN_{em}/dt is caused by the electric field enhancement by SF_6^+ ions in the vicinity of the cathode. The screening of FE is obtained at the time that coincides with the time of the VC formation $t_{VC} \approx 92$ ps. The total number of electrons N_e emitted and generated in the CA gap is shown also in Fig. 2(a). The value of N_e is controlled by two competitive processes: ionization and attachment of electrons to SF_6. In Fig. 2(b), one can see that both the ionization and attachment become dominant processes at different time intervals. At the beginning, when the space charge is relatively small and does not influence the electric field significantly, the ionization is the dominant process. Later, when the potential well OK*A [see Fig. 1(a)] is formed, the rate of ionization decreases and electron attachment becomes the dominant process. At 76 ps $< t <$ 198 ps, the ionization dominates over the attachment again and at larger times the attachment process slightly exceeds ionization with a tendency to be balanced by the ionization. The higher rate of attachment process causes a decrease in N_e at $t >$ 200 ps [see Fig. 2(a)].

The time evolution of numbers of RAE in the entire CA gap with $\varepsilon_e \geq 1$ and $\varepsilon_e \geq 20$ keV are presented in Fig. 3(a). Here let us note that in the results of simulations all the electrons with $\varepsilon_e \geq 1$ keV were considered as RAE because general criterion for RAE generation was fulfilled at different locations inside the CA gap in the case of strongly nonuniform electric field. Also, the generation of RAE with $\varepsilon_e \geq 20$ keV was studied separately, since, as shown below, VC formation influences in different ways on generation of RAE with $\varepsilon_e \geq 1$ and $\varepsilon_e \geq 20$ keV. One can see that the termination of the generation of RAE with $\varepsilon_e \geq 1$ keV that occurs at ~92 ps coincides with the times of FE screening and VC formation. The generation of RAE with $\varepsilon_e \geq 20$ keV continues during ~10 ps after the termination of the generation of

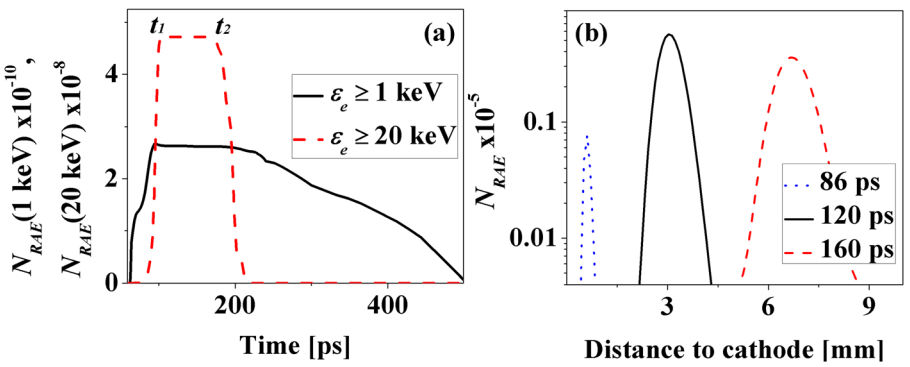

FIG. 3. (Color online) (a) Time dependence of the quantity of the RAE with $\varepsilon_e \geq 1$ and $\varepsilon_e \geq 20$ keV inside the CA gap; (b) space distribution of electrons with $\varepsilon_e \geq 20$ keV at different times; $\varphi_0 = 120$ kV, $T = 1$ ns, $P = 10^5$ Pa.

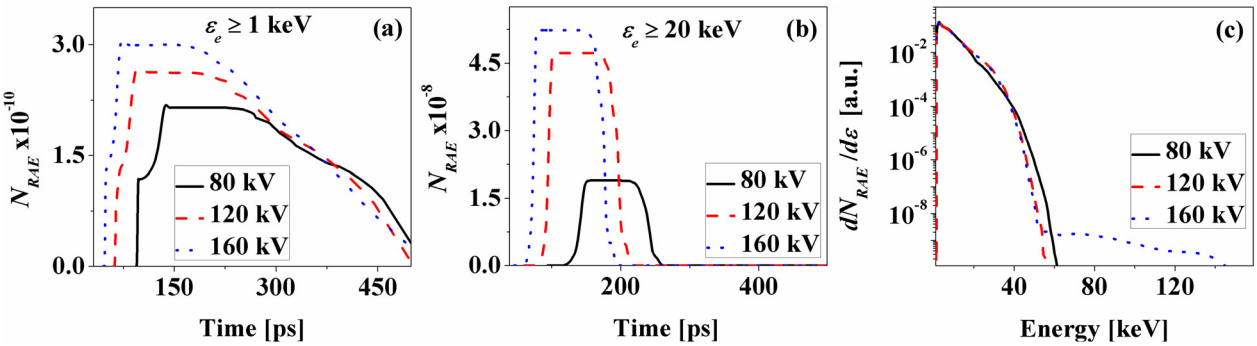

FIG. 4. (Color online) Time dependence of RAE number for different amplitudes of cathode potential: (a) N_{RAE} with $\varepsilon_e \geq 1$ keV, and (b) N_{RAE} with $\varepsilon_e \geq 20$ keV; (c) EEDF at the anode at $t = 0.5$ ns for different amplitudes of cathode potential; $T = 1$ ns; $P = 10^5$ Pa.

RAE with $\varepsilon_e \geq 1$ keV. The latter is explained by the part of the RAE with $1\,\text{keV} \leq \varepsilon_e < 20\,\text{keV}$ gaining energy in the electric field and contributing it to the RAE with $\varepsilon_e \geq 20$ keV. In addition, the generation of such RAE begins and terminates during the HV pulse rise time. The time interval $t_1 \leq t \leq t_2$ [see Fig. 3(a)], where the number of RAE with $\varepsilon_e \geq 20$ keV is constant, corresponds to the time when these RAE have not yet reached the anode. The space distribution (space resolution of 10^{-3} cm) of energetic electrons ($\varepsilon_e \geq 20$ keV) in this bunch inside the CA gap for different times is presented in Fig. 3(b). This bunch consists of the RAE generated prior the formation of the VC, which consists mainly of SF_6^- and, therefore, the VC is not an effective source of RAE with $\varepsilon_e \geq 20$ keV, although it generates a small amount of RAE with the energies of a few keV.

The simulations showed that the increase in the value of φ_0 increases slightly the VC potential and decreases the time of the VC formation. It was obtained that for $\varphi_0 = 80$ kV the VC formed with $\varphi_{VC} \approx -60$ kV at $t_{VC} \approx 134$ ps, for $\varphi_0 = 120$ kV one obtains $\varphi_{VC} \approx -64$ kV at $t_{VC} \approx 89$ ps, and for $\varphi_0 = 160$ kV one obtains $\varphi_{VC} \approx -67$ kV at $t_{VC} \approx 73$ ps. On the one hand, the faster VC formation causes the faster termination of RAE generation. Thus, the increase in the cathode potential decreases the duration of RAE which agrees with the experimental results presented in Ref. 7. On the other hand, the increase in φ_0 value at constant HV pulse rise time increases the dN_{em}/dt and more electrons become RAE [see Figs. 4(a) and 4(b)]. In addition, it is important to note that the distance between cathode and VC does not depend noticeably on φ_0 and is equal to $r_{VC} \approx 0.04$ mm (in the N_2-filled diode this effect was not obtained[7]). An insignificant dependence of $\varphi_{VC} = f(\varphi_0)$ indicates that the electric field distribution in the CA gap is qualitatively almost similar for $\varphi_0 = 80$, 120, and 160 kV. Therefore, the rate of ionization has approximately equal values at the same CA locations at different values of φ_0 and, respectively, the maximum of negative charge density is the same at different φ_0. Indeed, the simulation showed that the position of $(\rho_- - \rho_+)$ maximum does not depend on φ_0, i.e., the value of r_{VC} also does not depend on φ_0.

Normalized electron energy distribution functions (EEDF) for electrons reaching the anode with energy $\varepsilon_e \geq 1$ keV within a time interval between the $t = 0$ and $t = T/2$ for different values of φ_0 are shown in Fig. 4(c). One can see that the spectra for all values of φ_0 do not differ significantly at $\varepsilon_e < 60$ keV, while the EEDF for $\varphi_0 = 160$ kV contains more electrons in its high-energy tail.

The increase in the SF_6 gas pressure decreases the values of t_{VC}, φ_{VC}, and r_{VC}. Simulations showed that $\varphi_{VC} \approx -76$ kV, $t_{VC} \approx 109$ ps, $r_{VC} \approx 0.05$ mm for $P = 0.5 \times 10^5$ Pa, $\varphi_{VC} \approx -64$ kV, $t_{VC} \approx 89$ ps, $r_{VC} \approx 0.04$ mm for $P = 10^5$ Pa, and $\varphi_{VC} \approx -60$ kV, $t_{VC} \approx 80$ ps, $r_{VC} \approx 0.02$ mm for $P = 1.5 \times 10^5$ Pa. Therefore, the increase in pressure decreases both N_{RAE} and the time of the termination of RAE generation [see Fig. 5(a)]. The first result agrees with the results of experiments presented in Ref. 7. In addition, increased pressure decreases the RAE number in the high-energy tail of EEDF [see Fig. 5(b)].

The time dependences of the number of RAE in the CA gap with $\varepsilon_e \geq 20$ keV at different HV pulse rise times are presented in Fig. 5(c). One can see that the increase in $T/4$ increases the time of RAE termination although it decreases the total RAE number. The first dependence is caused by the longer time of VC formation, namely, the simulations showed that $t_{VC} \approx 89$ ps at $T = 1$ ns, $t_{VC} \approx 127$ ps at $T = 1.5$ ns, and $t_{VC} \approx 310$ ps at $T = 2$ ns. The decrease in total RAE number is caused by less intense FE at smaller T. Figure 5(d) shows that the EEDFs at the anode at $T = 1$ and $T = 1.5$ ns do not

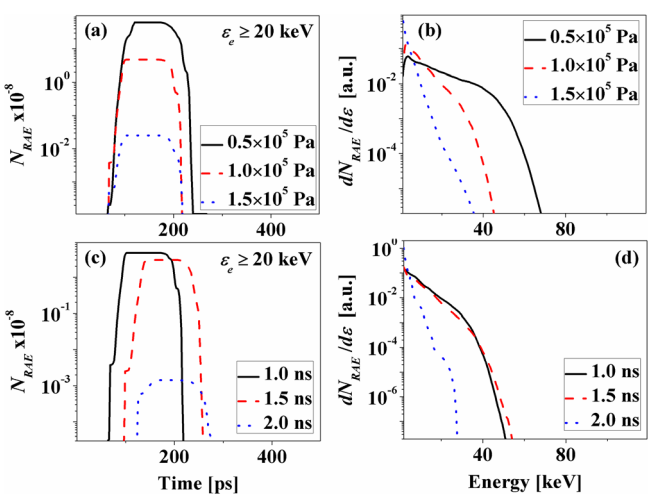

FIG. 5. (Color online) Time dependence of the RAE number with $\varepsilon_e \geq 20$ keV at different SF_6 pressures (a) and different HV pulse rise times (c) for $T = 1$ ns and $\varphi_0 = 120$ kV; EEDF at the anode at different SF_6 pressures (b) and different HV rise times (d) for $P = 10^5$ Pa and $\varphi_0 = 120$ kV.

differ significantly, and the main part of electrons at $T = 2$ ns has $\varepsilon_e < 20$ keV and the largest electrons energy is ≈ 28 keV.

IV. SUMMARY

The results of 1D PIC numerical simulation of RAE generation in electronegative SF_6 gas are presented. It was shown that the RAE generation is strongly influenced by the formation of the VC. The VC formation is governed by the attachments of low-energy electrons to SF_6 molecules. It was shown that the RAE are mainly the electrons emitted from the cathode and generated in the cathode vicinity. The generation of RAE is terminated with the formation of the VC, which screens FE.

It was shown that the RAE parameters depend on the initial conditions, such as the amplitude and rise time of the HV pulse and gas pressure. An increase in HV amplitude increases the VC potential while decreasing the time of its formation. The latter leads to an increase in the number of RAE and a decrease in the time of termination of RAE generation. In addition, it was shown that the EEDF obtained at the anode contains electrons with $\varepsilon_e < e\varphi_0$.

The increase in SF_6 gas pressure causes the decrease in both the time of the VC formation and its potential. These effects led to a decrease in both the RAE number and the time of termination of its generation. Also, the increase in the gas pressure decreases both the number of RAE in the high-energy tail of EEDF and the highest obtaining electrons energy. The increase in the HV pulse rise time increases the time of termination of RAE generation, and decreases both the total number of RAE and the number of RAE in the high-energy tail of EEDF.

ACKNOWLEDGMENTS

This work was supported in part at the Technion by a fellowship from the Lady Davis Foundation.

[1]G. A. Mesyats, V. V. Osipov, and V. F. Tarasenko, *Pulsed Gas Laser* (SPIE, Washington, 1995).
[2]L. P. Babich, T. V. Loiko, and V. A. Tsukerman, Physics–Uspekhi **33**, 521 (1990) and references therein.
[3]Y. D. Korolev and G. A. Mesyats, *The Physics of Pulse Breakdown* (Nauka, Moscow, in Russian, 1991).
[4]V. F. Tarasenko and S. I. Yakovlenko, Physics–Uspekhi **47**, 887 (2004) and references therein.
[5]A. M. Boichenko, A. N. Tkachev, and S. I. Yakovlenko, JETP Letters **78**, 709 (2003).
[6]A. N. Tkachev and S. I. Yakovlenko, Laser Physics **12**, 1022 (2002), available on-line at http://www.maik.ru/full/lasphys/02/7/lasphys7_02p1022full.pdf
[7]E. Kh. Baksht, A. G. Burachenko, M. V. Erofeev, M. I. Lomaev, D. V. Rybka, D. A. Sorokin, and V. F. Tarasenko, Laser Physics **18**, 732 (2008).
[8]D. Levko, S. Yatom, V. Vekselman, J. Z. Gleizer, V. Tz. Gurovich, and Ya. E. Krasik, "Numerical simulations of runaway electron generation in pressurized gases," J. Appl. Phys. (to be published).
[9]H. Itoh, Y. Miura, N. Ikuta, Y. Nakao, and H. Tagashira, J. Phys. D: Appl. Phys. **21**, 922 (1988).
[10]*NIST*: Electron-Impact *Cross Section* Database at http://physics.nist.gov/PhysRefData/Ionization/Xsection.html.
[11]Y. P. Raizer, *Gas Discharge Physics* (Springer, Berlin, 1991).